ANALYSIS OF THE CRYSTAL STRUCTURE AND ENERGY FRAMEWORKS OF 5-ACETIL-1,3-DIMETHYL BARBITURIC ACID

Sultan KINCAL*, Faculty of Science, Department of Chemistry, Mugla Sıtkı Koçman University, Mugla, sultankincal@mu.edu.tr
(https://orcid.org/0000-0003-3865-9671)
Cansu TOPKAYA, Faculty of Science, Department of Chemistry, Mugla Sıtkı Koçman University, Mugla, cansutopkaya@mu.edu.tr
(https://orcid.org/0000-0002-6834-4841)
Ramazan GÜP, Faculty of Science, Department of Chemistry, Mugla Sıtkı Koçman University, Mugla, rgup@mu.edu.tr
(https://orcid.org/0000-0001-5731-6733)
Tuncer HÖKELEK, Faculty of Science, Department of Physics, Hacettepe University, Ankara, merzifon@hacettepe.edu.tr
(https://orcid.org/0000-0002-8602-4382)

Abstract

$C_8H_9N_2O_4$ was prepared via acetylation of 1,3-dimethyl barbituric acid. The atomic and crystalline structures were determined using single crystal analysis (X-ray). It is a member of the monoclinic system P 2_1/c group of space with a = 8.6056 (3) Å, b = 9.1602 (3) Å, c = 11.9601 (4) Å, β = 109.410 (3)°, Z = 4 and V = 889.22 (5) $Å^3$.

π–π interactions between circles of nearby molecules with intercentroid distances of 3.4300 (11) aid in the stability of the structure by keeping the crystals in place. The Hirshfeld surface (HS) analysis of the crystal structure reveals that the H...O/O...H (45.9%) and H...H (32.9%) interactions contribute the most to crystal packing. The most essential interactions in crystal packing are hydrogen bonding and van der Waals interactions. According to the dispersion, electrostatic and overall energy frameworks, the contribution of dispersion energy dominates the stability.

Keywords: Barbituric acid, pyrimidine, crystal structure, energy framework, interaction energy.

5-ASETİL-1,3-DİMETİL BARBİTÜRİK ASİTİN KRİSTAL YAPISININ ve ENERJİ DAĞILIMLARININ ANALİZİ

Özet

Başlıkta sözü edilen bileşik, $C_8H_9N_2O_4$, 1,3-dimetil barbitürik asidin asetilasyonu yoluyla sentezlenmiştir. Molekülün kristal yapısı tek kristal X-ışını analizi ile ortaya koyularak, kristal yapının a = 8.6056 (3) Å, b = 9.1602 (3) Å, c = 11.9601 (4) Å, β = 109.410 (3)°, Z = 4 ve V = 889.22 (5) Å3 değerleri ile monoklinik sistem, P 21/c uzay grubu olduğu bulunmuştur.

Kristal yapıda, π–π etkileşimleri [3.4300(11) Å'lik merkezler arası mesafelere sahip bitişik moleküllerin halkaları arasındaki] kristal paketlemenin pekiştirilmesine yardımcı olur. Kristal yapının Hirshfeld yüzey analizi, kristal yapının kristal paketleme için en önemli katkılarının H...O/O...H (% 45.9) ve H...H (% 32.9) etkileşimlerinde olduğunu gösterir. Hidrojen bağı ve van der Waals etkileşimleri, kristal paketlemedeki baskın etkileşimlerdir. Elektrostatik, dağılım ve toplam enerji dağılımlarının değerlendirilmesi sonucu, stabilizasyonda dağılım enerjisi katkısının daha baskın olduğunu görülmüştür.

Keywords: Barbiturik asit, primidin, kristal yapı, enerji dağılımı, etkileşim enerjisi.

Cite

1. Introduction

Pyrimidine compounds are a class of heterocyclic compounds that have two nitrogen atoms in their structure. Barbituric acid, a member of the pyrimidine class and also its derivatives products have been proven to have various biological and pharmacological activities. [1-12]

Methods for the acetylation of barbituric acid derivatives have been established that are both efficient and simple. [12] The acetylated barbituric acid derivatives obtained as a result of synthesis can be converted into highly efficient Schiff bases by condensation reactions and as a starting compound for the synthesis of coordination compounds. [13-19]Thus, they can form monodentate or polydentate ligands that offer different bonding sites with the electron donating atoms in their structure. [14-

19]These coordination compounds synthesized with acetylated pyrimidine derivatives have been the subject of many studies due to their antitumor, anti-cancer, anti-osteoporp-free, antimicrobial, anti-inflammatory, antitubercular, anticonvulsant interactions.[7,20-33]

In this study, X-ray quality crystals were obtained after acetylation steps of 1,3 dimethylbarbituric acid compound. The molecular and crystal structures of 5-acetyl-1,3 dimethylbarbituric acid (1,3-ABA) were investigated using single crystal analysis, X-ray diffraction technique and various spectroscopic techniques. Then, the HS analysis of the compound was made and the electrostatic, distribution and overall energy frameworks were evaluated.

2. Experimental

2.1. Materials and measurements

Solvents and chemicals used in the laboratory were obtained commercially from manufacturers Merck and Sigma. Solvents used in synthesis and measurements were freshly distilled and dried according to the appropriate procedure. Analysis of elements (C, N, H) were accomplished on a LECO 932 CHNS analyzer. [1H] NMR spectrum of the samples were collected on a Bruker 400 MHz spectrometer in DMSO_d_6. From 4000 to 400 cm^{-1}, an FTIR spectrum was obtained on a pure solid sample with a Thermo-Scientific Nicolet iS10-ATR utilizing the ATR (attenuated total reflectance) method on a Thermo-Scientific Nicolet iS10-ATR. Electrothermal IA 9100 (UK) digital melting point equipment was used to determine the melting point. A PG Instruments T80+ UV/Vis Spectrophotometer was used to acquire the electronic spectrum. Crystal structures data were recorded using Mo K radiation (= 0.71073) at 296(2) K on a Bruker APEX-II CCD diffractometer.

2.2. Synthesis and characterization

1,3-ABA [12] were synthesized as previously reported in the literature (Scheme 1). X-ray quality crystals obtained from acetone and water by slow vaporization at 25 °C.
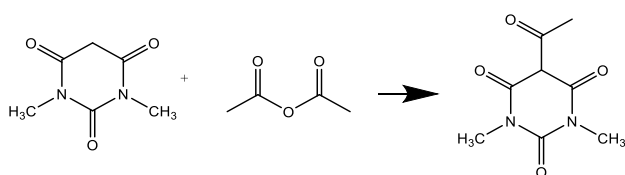
Scheme 1. Synthesis of 1,3-ABA

5-acetyl-1,3-dimethyl barbituric acid : Light yellow solid, yield: 85%, M. P.: 92 °C. FTIR (ATR, cm[-1]): 2963, 2928 ν(-CH$_3$), 1722, 1656, 1690 ν(C=O), 1221 ν(C-O). [1H] NMR (400 MHz, DMSO_d_6, ppm) δ 7.46 (s, 1H, Ar-H), δ 3.33 (s, 3H, -CH$_3$), δ 3.37 (s, 3H, -CH$_3$), δ 2.72 (s, 3H, -CH$_3$). Analysis (% calculated/found) for $C_8H_{10}N_2O_4$, C: 48.48/48.40, H: 5.09/5.01, N: 14.14/14.44.

2.3. X-ray crystallography

The ORTEP-3 [35] program was utilized in the drawings, and the SHELX software packages [SHELXS97 and SHELXL97] [34] were used to solve and improve the structure in the processing of crystallographic data.

The atomic locations of hydrogen were determined geometrically using distances of 0.96 (for CH3) and then corrected using a driving model that incorporated the mechanism of imposing restrictions to Uiso(H) = 1.5X Ueq (C).

3. Result and Discussion

3.1. Characterization of the compound

In the FTIR spectrum of 1,3- ABA, the carbonyl (C=O) peak was observed at 1722 cm^{-1}, which was appointed to the acetyl moiety and the C-O bending peak belonging to the same group was observed at 1221 cm^{-1}.These newly emerged peaks support that the barbituric acid compound has been successfully acetylated. Carbonyl peaks in the barbituric acid ring (C=O) were also observed intensely around 1656 and 1690 cm^{-1}.In addition, the peaks of the methyl (-CH$_3$) groups attached to the nitrogen atoms in the structure of the compound were observed around 2963 and 2928 cm^{-1}. [36, 37]

When the compound's [1H] NMR spectra is studied, it is seen that the peaks observed at 3.33 and 3.37 ppm belong to the (-N-CH$_3$) groups in the structure of the compound. The apex of the singlet observed at 7.46 ppm was determined to belong to the hydrogen (5-H) attached to the carbon atom 5, where the acetylation reaction took place. Hydrogens belonging to the methyl group formed as a result of acetylation, emerged as singlet at 2.72 ppm. [12,36,38] When all spectroscopic datas are evaluated together, it is seen that the acetylation reaction of 1,3-dimethylbarbituric acid has been successfully carried out.

3.2. X-Ray structure

The compound's X-ray structural assessment agrees with pertinent spectroscopic data and supports the structure. Experimental details used to illuminate the crystal structure are in Table 1; the lengths between some selected atoms are given in Table 2. The asymmetric unit of the structure obtained by numbering the atoms is shown in Fig. 1.

 Atoms O1, O2, O3, O4, C5, C6, C7 and C8 are –0.0128 (18) Å, –0.0813 (20) Å, 0.0392 (18) Å, –0.0867 (20) Å, –0.0875 (25) Å, –0.1862 (34) Å, –0.0182 (27) Å and 0.0369 (27) Å away from the best least-squares plane of ring *A* (N1/N2/C1—C4), respectively. So, atoms O1, O3, C7 and C8 are almost coplanar with ring *A*.

In the structure of crystal (Fig. 2), π–π interactions between the planar, *A* (N1/N2/C1—C4) rings, Cg1 … Cg1[i] of neighbouring molecules help to consolidate the crystal packing [distance between the centroids = 3.4300(11) Å; code of symmetry: (ii) – x, – y, – z; Cg1 is the center of ring *A* (N1/N2/C1—C4)].

Table 1. Experimental details.

Crystal data	
Formula for Chemical	$C_8H_9N_2O_4$
M_r	197.17
System of crystals, space class	Monoclinic, $P2_1/c$
Temperature (K)	296
a, b, c (Å)	8.6056 (3), 9.1602 (3), 11.9601 (4)
β (°)	109.410 (3)
V (Å³)	889.22 (5)
Z	4
Type of Radiation	Mo $K\alpha$
μ (mm⁻¹)	0.12
Crystal size (mm)	0.25 × 0.20 × 0.17
Gathering data	
Diffractometer	Bruker *APEX* II QUAZAR three-circle diffractometer
Correction of Absorption	–
The number of measurable, independent, and observable [$I > 2\sigma(I)$] reflections [$I > 2(I)$]	11043, 2033, 1395
R_{int}	0.053
$(\sin\theta/\lambda)_{max}$ (Å⁻¹)	0.649
Refining	
$R[F^2 > 2\sigma(F^2)]$, $wR(F^2)$, S	0.055, 0.179, 1.07
Number of reflections	2033
Number of parameters	130
H-atom treating	Constraints on H-atom parameters
$\Delta\rho_{max}$, $\Delta\rho_{min}$ (e Å⁻³)	0.34, −0.16

Computer programs: *APEX2* [39], *SAINT* [39], *SHELXS97*; [34] *SHELXL97*; [34], *ORTEP-3* for Windows [35], *WinGX* publication routines [35] and *PLATON* [40]
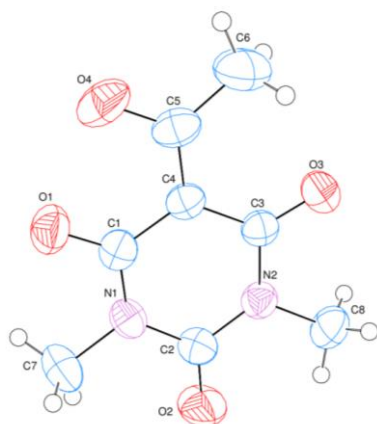
Figure 1. The asymmetric unit of 1,3-ABA that has a numbered atom system. The %50 probability level is used to design thermal ellipsoids.
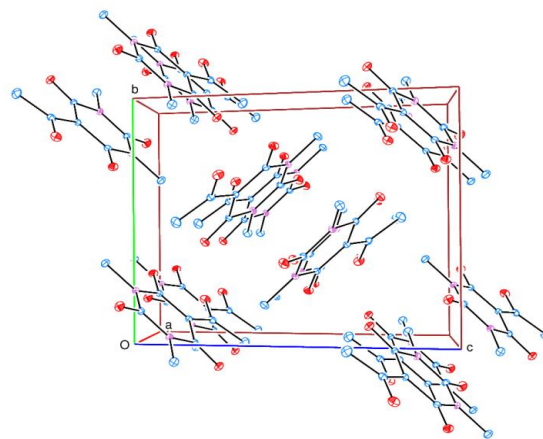
Figure 2. A packing diagram with the hydrogen atoms removed, based on the A-axis.

3.3. Hirshfeld surface analysis

A analysis of HS [41,42] was done using Crystal Explorer 17.5[43] to show the intermolecular interactions in the crystal structure of the molecule. As a result of the research, the white surface on the Dnorm (Fig. 3) reveals connections with lengths equal to the total of the van der Waals radii. Shorter (in close contact) van der Waals radii are indicated by red hues, whereas longer (specific contact) distances are indicated by blue colors [44].
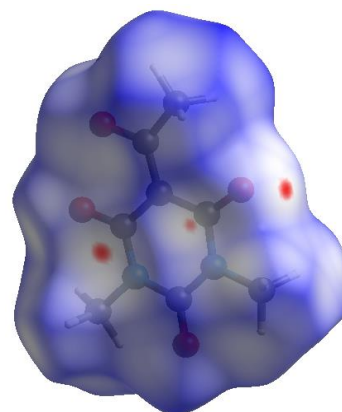
Figure 3. Three-dimensional HS view of the compound obtained by plotting on the dnorm in the scale of -0.0370 to 1.0433 a.u.

The bright red spots on the picture represent the respective donors and/or acceptors; the blue and red regions in Fig. 4 represent positive and negative potentials on the HS linked using the electrostatic potential [45,46].

Blue sections show positive electrical potential (H-bonded donors), whereas red sections indicate negative electrical potential (H-bonded acceptors).

The shapes and colors used in HS analysis are interpreted as follows. The presence of adjacent red and blue triangons is an image used to envision the π...π stack in the molecule. If the study determines that there are no surrounding red and/or blue triangular piece, there is no π...π interaction in the molecule. Figure 5 clearly shows that there are π...π interactions in (I).
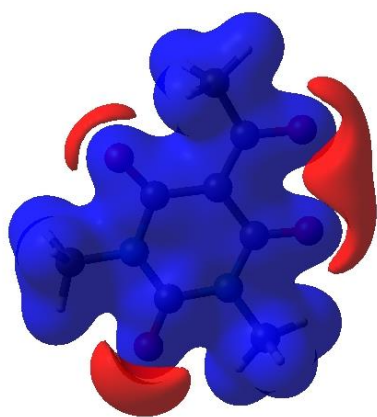
Figure 4. The shape of the three-dimensional HS of the compound. This figure is drawn using the Hartree-Fock theory and the STO-3 G basis tuned at electrostatic potential energy in the scale of -0.0500-0.0500 a.u. Blue and red patches represent hydrogen bond donors and acceptors, respectively.
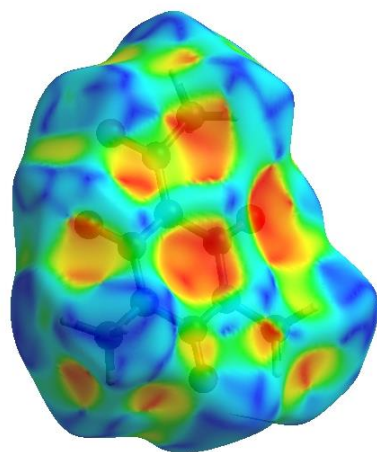
Figure 5. The HS drawn on the shape index of the compound.

In general, fingerprint layout in two dimensions, Fig. 6*a*, and those delineated into H...O/O...H, H...H, H...C/C...H, O...C/C...O, N...C/C...N, C...C, O...N/N...O, O...O and H...N/N...H [47] are illustrated in Figs. 6*b—j*, respectively, as well as their proportional additives to the HS. Almost all crucial interaction is the H...O/O...H contacts (Table 2), which contribute 45.9% to the overall crystal packing, and Figure 6b shows that the hints are also projected as spikes of symmetrical distribution with $d_e + d_i = 2.75$ Å = 2.56 Å. The H...H interactions are depicted in Fig. 6c as dense and widely spread patches arising from the molecule's high hydrogen content ($d_e = d_i = 1.17$).

If there isn't any interactions between C—H...π, a characteristic pair of blades (Fig. 6d, 6.9% contribution to HS) expressed as H...C/C...H (Table 2) in the fingerprint plan contacts also has hints at $d_e + d_i = 2.75$ Å. Table 2 shows a distribution that is symmetrical of dots with the pair of wings at $d_e + d_i = 3.17$ for the O...C/C...O (4.4 percent, Fig. 6e) connections. The N...C/C...N (3.8%, Fig. 6f) and C...C (2.2%, Fig. 6g) contacts have bullet-shaped and arrow-shaped distributions of dots with the hints at

$d_e = d_i = 1.70$Å and $d_e = d_i = 1.74$ Å, respectively. Finally, the O...N/N...O (1.5 percent, Fig. 6h), O...O (1.4 percent, Fig. 6i), and H...N/N...H (1.0 percent, Fig. 6j) connections feature distributed low-density dots with hints at $d_e + d_i$ = 3.08, 1.85, and 3.00, separately.

Table 2. Interatomic distances of interest (Å).

O1⋯O4	2.429 (3)	O2⋯H7A	2.35
O3⋯C6	2.807 (3)	O3⋯H6B	2.62
O3⋯C1[i]	3.165 (3)	O3⋯H8A	2.66
O1⋯H8A[ii]	2.72	O3⋯H8C	2.63
O1⋯H7B	2.39	O3⋯H6C	2.54
O1⋯H7C[iii]	2.72	H7B⋯C3[v]	2.84
O2⋯H8B	2.26	H8C⋯C7[vi]	2.89
O2⋯H8B[iv]	2.63		

Symmetry codes: (i) –*x*, *y*–1/2, –*z*+1/2; (ii) –*x*, –*y*, –*z*; (iii) –*x*, –*y*+1, –*z*; (iv) –*x*–1, –*y*, –*z*; (v) *x*, –*y*+1/2, *z*–1/2; (vi) *x*, –*y*+1/2, *z*+1/2.
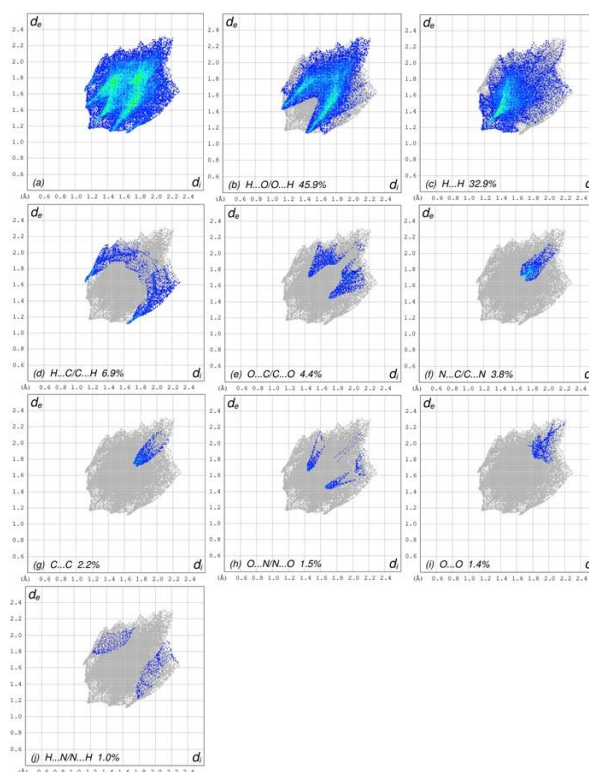
Figure 6. The entire two-dimensional fingerprinting plots for the molecule, demarcated into (a) H...O/O...H, (b) H...H, (c) H...C/C...H, (e) O...C/C...O, (f) N...C/C...N, (g) C...C, (h) O...N/N...O, I O...O, and (j) H...N/N...H connections. The d_i and d_e values in Å are the closest inner and outer distances from the specified dots on the HS interactions.

In Figs. 7 a,b, the HS declarations with the mission dnorm plotted onto the surface for the H...O/O...H and H...H interactions are presented.

HS analyzes highlight the importance of H-atom interactions in the formation of the packing. Van der Waals interactions and hydrogen bonding play key roles in crystal packing, as evidenced by the presence of multiple H...O/O...H and H...H interactions [48].
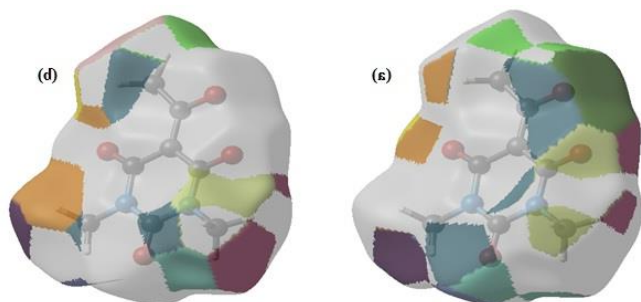
Figure 7. For (a) H...H, (b) H...O/O...H, and (c) H...C/C...H interactions, the HS declarations with the mission dnorm mapped onto the surface.

3.4. Interaction energy calculations

The model of energy CE–B3LYP/6–31G(d,p) found in Crystal Explorer 17.5 [43] is used to determine intermolecular interaction energies. A collection of compounds is created in this computation by performing crystallographic symmetry operations on a specified core molecule with a radius of 38 [49].

The overall intermolecular energy is calculated by adding the electrostatic (E_{ele}), polarization (E_{pol}), dispersion (E_{dis}), and exchange-repulsion (E_{rep}) energies(E_{tot}) [50], with scale factors of 1.057, 0.740, 0.871, and 0.618, separately [51].

3.5. Energy frameworks

The computation of intermolecular interaction energies, as well as a graphical depiction of their magnitude, are referred to as energy frameworks [50]. The energies between molecule pairs are represented by cylinders that connect their centers of gravity, with the radius of the cylinder proportional to the relative intensity of the associated interaction energy.

E_{ele} (red rollers), E_{dis} (green rollers) and E_{tot} (blue rollers) all have their own energy frameworks (Fig. 8). After examining energy frameworks of the electrostatic, dispersion, and overall, it is clear that dispersion energy plays the most important and effective role in stability.
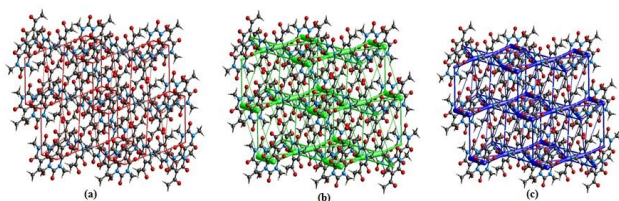
Figure 8. Diagrams of electrostatic energy(a), dispersion energy(b), and overall energy(c) are all perspectives on the energy framework for a group of

molecules. In 2 X 1 X 2 unit cells, the cylindrical radius is proportional to the relative intensity of the associated energies and is set to the same scale factor of 80 with a cut off of 5.

4. Conclusion

This article discusses the synthesis and characterisation of 5-acetyl-1,3-dimethyl barbituric acid, as well as HS analysis, computation of interaction energies, and energy frameworks. Single crystal analysis (X-ray) was used to determine the structure of the substance, and the results were corroborated by spectroscopic investigation. HS study reveals the critical role of H-atom interactions in the forming structure. Furthermore, it demonstrates that van der Waals and hydrogen bonds interactions are critical for crystal packing. When the electrostatic, dispersion, and overall energy frameworks were evaluated, it was determined that the dispersion energy contribution to the stabilization of the compund was significant.

5. Acknowledgment

6. References

[1] Gulliya, K. S. (1997). *U.S. Patent No. 5,674,870*. Washington, DC: U.S. Patent and Trademark Office.

[2] Oliva, A., De Cillis, G., Grams, F., Livi, V., Zimmermann, G., Menta, E., & Krell, H. W. (2002). *U.S. Patent No. 6,335,332*. Washington, DC: U.S. Patent and Trademark Office.

[3] Rastaldo, R., Penna, C. and Pagliaro, P., ''Comparison between the effects of pentobarbital or ketamine/nitrous oxide anesthesia on metabolic and endothelial components of coronary reactive hyperemia'', *Life Sciences*, 69(6), 729-738, 2001.

[4] Aiken, S. P. and Brown, W. M., ''Treatment of epilepsy: existing therapies and future developments'', *Front Biosci*, 5(1), E124-52, 2000.

[5] Ghansah, E. and Weiss, D. S., '' Modulation of GABAA receptors by benzodiazepines and barbiturates is autonomous of PKC activation'', *Neuropharmacology*, 40(3), 327-333, 2001.

[6] Ma, L., Li, S., Zheng, H., Chen, J., Lin, L., Ye, X. and Chen, L., ''Synthesis and biological activity of novel barbituric and thiobarbituric acid derivatives against non-alcoholic fatty liver disease'', *European journal of medicinal chemistry*, 46(6), 2003-2010, 2011.

[7] Laxmi, S. V., Janardhan, B., Rajitha, B., Raghavaiah, P. and Srinivas, P., ''Synthesis, single crystal X-ray studies and antimicrobial activities of novel Indole barbiturates'', *Medicinal Chemistry Research*, 21(10), 2896-2901, 2012.

[8] Palwinder, S., Matinder, K. and Pooja, V., ''Design, synthesis and anticancer activities of hybrids of indole and barbituric acids—Identification of highly promising leads'', *Bioorg Med Chem Lett*, 19, 3054-3058, 2009.

[9] Shiradkar, M. R., Ghodake, M., Bothara, K. G., Bhandari, S. V., Nikalje, A., Akula, K. C. and Burange, P. J., ''Synthesis and anticonvulsant activity of clubbed thiazolidinone–barbituric acid and thiazolidinone–triazole derivatives'', *Arkivoc*, 14, 58-74, 2007.

[10] Goodman, L.S, Gilman, A., *The pharmacological basis of therapeutics,* The Macmillan,1975.

[11] Giziroglu, E., Aygün, M., Sarikurkcu, C., Kazar, D., Orhan, N., Firinci, E. and Gokcen, C., ''Synthesis, characterization and antioxidant activity of new dibasic tridentate ligands: X-ray crystal structures of DMSO adducts of 1, 3-dimethyl-5-acetyl-barbituric acid o-hydroxybenzoyl hydrazone copper (II) complex'', *Inorganic Chemistry Communications*, 36, 199-205, 2013.

[12] Jursic, B. S. and Neumann, D. M., ''Preparation of 5-formyl- and 5-acetylbarbituric acids, including the corresponding Schiff bases and phenylhydrazones'', *Tetrahedron Letters*, 42(48), 8435-8439,2001.

[13] Gup, R. and Giziroğlu, E., ''Metal complexes and solvent extraction properties of isonitrosoacetophenone 2-aminobenzoylhydrazone'', *Spectrochimica Acta Part A: Molecular and Biomolecular Spectroscopy*, 65(3-4), 719-726, 2006.

[14] Kaminsky, W., Jasinski, J. P., Woudenberg, R., Goldberg, K. I. and West, D. X., ''Structural study of two N (4)-substituted thiosemicarbazones prepared from 1-phenyl-1, 2-propanedione-2-oxime and their binuclear nickel (II) complexes'', *Journal of molecular structure*, 608(2-3), 135-141, 2002.

[15] Bertrand, J. A., Smith, J. H. and Eller, P. G. ''Crystal and molecular structure of bis {perchlorato [2-(2-hydroxyethyl) imino-3-oximobutanato] aquocopper (II)}. Copper (II) dimer with bridging oxime groups'', *Inorganic Chemistry*, 13(7), 1649-1653,1974.

[16] Butcher, R. J., O'Connor, C. J. and Sinn, E., ''Synthesis and relation between magnetism and structure of the binuclear copper (II) oxime complex [Cu2L2 (ClO4) 2].[Cu2L2 (CH3OH) 2](ClO4) 2, where HL= 1-(N, N-dimethyl-2-aminoethylimino)-1-phenyl-2-oximopropane'', *Inorganic Chemistry*, 18(7), 1913-1918, 1979.

[17] Abraham, F., Capon, J. M., Nowogrocki, G., Sueur, S. and Bremard, C.,''Synthesis, X-ray structure and spectroscopy of Cu (II) complexes derived from diacetylazine dioxime'', *Polyhedron*, 4(10), 1761-1767,1985.

[18] Maekawa, M., Kitagawa, S., Nakao, Y., Sakamoto, S., Yatani, A., Mori, W. and Munakata, M., ''Syntheses, crystal structures and autoreduction behavior of antiferromagnetically coupled dicopper (II) oximato complexes'', *Inorganica chimica acta*, 293(1), 20-29, 1999.

[19] Wan, S. P., Mori, W. and Yamada, S., ''Synthesis and properties of iodinated nickel imineoximes'', *Synthesis and Reactivity in Inorganic and Metal-Organic Chemistry*, 16(9), 1273-1288, 1986.

[20] A Angelusiu, M. V., Barbuceanu, S. F., Draghici, C. and Almajan, G. L.,''New Cu (II), Co (II), Ni (II) complexes with aroyl-hydrazone based ligand. Synthesis, spectroscopic characterization and in vitro antibacterial evaluation'', *European journal of medicinal chemistry*, 45(5), 2055-2062, 2010.

[21] Savini, L., Chiasserini, L., Gaeta, A. and Pellerano, C., ''Synthesis and anti-tubercular evaluation of 4-quinolylhydrazones'', *Bioorganic & medicinal chemistry*, 10(7), 2193-2198,2002.

[22] Giziroglua, E., Sarikurkcub, C. and Saracc, N., ''Synthesis and characterization of novel Hydrazone based anti-mutagenic and Antioxidative agents'', *Journal of Applied Pharmaceutical Science*, 5(3), 048-055, 2015.

[23] A Chugunova, E., D Voloshina, A., E Mukhamatdinova, R., V Serkov, I., N Proshin, A., M Gibadullina, E. and Goumont, R., '' The study of the biological activity of amino-substituted benzofuroxans'', *Letters in Drug Design & Discovery*, 11(4), 502-512, 2014.

[24] Glinma, B., Gbaguıdı, F. A., Urbain, C. K., Κρονιεσσı, S. D., Houngbeme, A., Houngue, H. D. And Poupaert, J. H., ''Synthesis and trypanocidal activity of salicylhydrazones and p-tosylhydrazones of S-(+)-carvone and arylketones on African trypanosomiasis'',*Journal of Applied Pharmaceutical Science*, 5(06), 001-007, 2015.

[25] Mahmudov, K. T., Kopylovich, M. N., Maharramov, A. M., Kurbanova, M. M., Gurbanov, A. V. and Pombeiro, A. J., ''Barbituric acids as a useful tool for the construction of coordination and supramolecular compounds'', *Coordination Chemistry Reviews*, 265, 1-37, 2014.

[26] Bojarski, J. T., Mokrosz, J. L., Bartoń, H. J. and Paluchowska, M. H.,''Recent progress in barbituric acid chemistry'', *Advances in heterocyclic chemistry*, 38, 229-297,1985.

[27] Patrick, G. L., *An introduction to medicinal chemistry*, Oxford university press.,2013.

[28] Parvathy, K. S., Negi, P. S. and Srinivas, P., ''Curcumin–amino acid conjugates: synthesis, antioxidant and antimutagenic attributes'', *Food Chemistry*, 120(2), 523-530, 2010.

[29] Abele, E., Abele, R., Golomba, L., Višņevska, J., Beresneva, T., Rubina, K. and Lukevics, E., ''Oximes of six-membered heterocyclic compounds with two and three heteroatoms. II.* Reactions and biological activity'', *Chemistry of heterocyclic compounds*, 46(8), 905-930,2010.

[30] Neumann, D. M., Cammarata, A., Backes, G., Palmer, G. E. and Jursic, B. S., ''Synthesis and antifungal activity of substituted 2, 4, 6-pyrimidinetrione carbaldehyde hydrazones'', *Bioorganic & medicinal chemistry*, 22(2), 813-826,2014.

[31] Zheng, L. W., Li, Y., Ge, D., Zhao, B. X., Liu, Y. R., Lv, H. S. and Miao, J. Y., ''Synthesis of novel oxime-containing pyrazole derivatives and discovery of regulators for apoptosis and autophagy in A549 lung cancer cells'' *Bioorganic & medicinal chemistry letters*, 20(16), 4766-4770, 2010.

[32] Dörwald, F. Z., Lead optimization for medicinal chemists: pharmacokinetic properties of functional groups and organic compounds. John Wiley & Sons, 2012.

[33] Khan, K. M., Khan, M., Ali, M., Taha, M., Hameed, A., Ali, S. and Choudhary, M. I., ''Synthesis and DPPH radical scavenging activity of 5-arylidene-N, N-dimethylbarbiturates'', *Medicinal Chemistry (Shariqah (United Arab Emirates))*, 7(3), 231-236, 2011.

[34] Sheldrick, G. M., ''A short history of SHELX'', *Acta Crystallographica Section A: Foundations of Crystallography*, 64(1), 112-122, 2008.

[35] Farrugia, L. J., ''WinGX and ORTEP for Windows: an update'', *Journal of Applied Crystallography*, 45(4), 849-854, 2012.

[36] Gup, R., Giziroglu, E. and Kırkan, B., ''Synthesis and spectroscopic properties of new azo-dyes and azo-metal complexes derived from barbituric acid and aminoquinoline'', *Dyes and pigments*, 73(1), 40-46, 2007.

[37] Kirkan, B. and Gup, R., ''Synthesis of new azo dyes and copper (II) complexes derived from barbituric acid and 4-aminobenzoylhydrazone'', *Turkish Journal of Chemistry*, 32(1), 9-17, 2008.

[38] Neumann, D. M., Cammarata, A., Backes, G., Palmer, G. E. and Jursic, B. S., ''Synthesis and antifungal activity of substituted 2, 4, 6-pyrimidinetrione carbaldehyde hydrazones'', *Bioorganic & medicinal chemistry*, 22(2), 813-826, 2014.

[39] Bruker, SMART and SAINT. Bruker AXS Inc., Madison, Wisconsin, USA, 2012.

[40] Spek, A. L., ''checkCIF validation ALERTS: what they mean and how to respond'', *Acta Crystallographica Section E: Crystallographic Communications*, 76(1), 1-11., 2020.

[41] Hirshfeld, F. L., ''Bonded-atom fragments for describing molecular charge densities'' *Theoretica chimica acta*, 44(2), 129-138, 1977.

[42] Spackman, M. A. and Jayatilaka, D., ''Hirshfeld surface analysis'', *CrystEngComm*, 11(1), 19-32, 2009.

[43] Turner, M. J., McKinnon, J. J., Wolff, S. K., Grimwood, D. J., Spackman, P. R., Jayatilaka, D. and Spackman, M. A., *CrystalExplorer17*. The University of Western Australia, 2017.

[44] Venkatesan, P., Thamotharan, S., Ilangovan, A., Liang, H. and Sundius, T., ''Crystal structure, Hirshfeld surfaces and DFT computation of NLO active (2E)-2-(ethoxycarbonyl)-3-[(1-methoxy-1-oxo-3-phenylpropan-2-yl) amino] prop-2-enoic acid'', *Spectrochimica Acta Part A: Molecular and Biomolecular Spectroscopy*, 153, 625-636, 2016.

[45] Spackman, M. A., McKinnon, J. J. and Jayatilaka, D., ''Electrostatic potentials mapped on Hirshfeld surfaces provide direct insight into intermolecular interactions in crystals'', *CrystEngComm*, 10(4), 377-388, 2008.

[46] Jayatilaka, D., Grimwood, D. J., Lee, A., Lemay, A., Russel, A. J., Taylor, C., Wolff, S. K., Cassam-Chenai, P. and Whitton, A., TONTO - A System for Computational Chemistry. Available at: http://hirshfeldsurface.net/, 2005.

[47] McKinnon, J. J., Jayatilaka, D. and Spackman, M. A., ''Towards quantitative analysis of intermolecular interactions with Hirshfeld surfaces'' *Chemical Communications*, (37), 3814-3816, 2007.

[48] Hathwar, V. R., Sist, M., Jørgensen, M. R., Mamakhel, A. H., Wang, X., Hoffmann, C. M. and Iversen, B. B., ''Quantitative analysis of intermolecular interactions in orthorhombic rubrene'', *IUCrJ*, 2(5), 563-574., 2015.

[49] Turner, M. J., Grabowsky, S., Jayatilaka, D. and Spackman, M. A., ''Accurate and efficient model energies for exploring intermolecular interactions in molecular crystals'' *The journal of physical chemistry letters*, 5(24), 4249-4255, 2014.

[50] Turner, M. J., Thomas, S. P., Shi, M. W., Jayatilaka, D. and Spackman, M. A., ''Energy frameworks: insights into interaction anisotropy and the mechanical properties of molecular crystals'', *Chemical Communications*, 51(18), 3735-3738, 2015.

[51] Mackenzie, C. F., Spackman, P. R., Jayatilaka, D. and Spackman, M. A., ''CrystalExplorer model energies and energy frameworks: extension to metal coordination compounds, organic salts, solvates and open-shell systems'', *IUCrJ*, 4(5), 575-587, 2017.